

TOXICITY ASSESSMENT OF BIOSYNTHEZED SILVER NANOPARTICLES FROM *SOLANUM VILLOSUM* MILL. (SOLANACEAE): *IN VITRO* AND *IN VIVO* STUDY

VENKATESH RAJENDRAN*, KALAIVANI KRISHNASAMY

Department of Biochemistry, Kongunadu Arts and Science College (Autonomous), Coimbatore - 641 029, Tamil Nadu, India.

Email: venkatbiochem11@gmail.com

Received: 29 September 2016, Revised and Accepted: 03 October 2016

ABSTRACT

Objective: The aim of the study is an evaluation of toxicity assessment of biosynthesized silver nanoparticles (AgNPs) from *Solanum villosum* (Mill.) using *in vitro* and *in vivo* study.

Methods: Biologically synthesized AgNPs are characterized by ultraviolet, scanning electron microscopy, energy dispersive X-ray spectroscopy, X-ray diffraction analysis, and its cytotoxicity effect against HepG2 cell lines was performed. Further, toxicity was confirmed by *in vivo* studies using Wistar albino rats. Various hematological, liver function marker enzymes and liver histopathology are investigated.

Results: The cytotoxic effect of *S. villosum* AgNPs (SV-AgNPs) was also concentration dependent and did not produce any toxicity to tested animals. The histopathological evidence is supported to biochemical observations.

Conclusion: So, biologically synthesized AgNPs are toxic only to cancer cells but not in animals were proved by the present study.

Keywords: *Solanum villosum* silver nanoparticles, HepG2 cell lines, Scanning electron microscopy, Energy dispersive X-ray spectroscopy, X-ray diffraction analysis.

INTRODUCTION

The field of nanotechnology is one of the upcoming areas of research in the modern field of material science. Nanoparticle shows completely new or improved properties, such as size, distribution, and morphology of the particles. Novel applications of nanoparticles and nanomaterials are emerging rapidly on various fields [1]. Nanocrystalline silver particles have been found tremendous applications in the fields of high sensitivity biomolecular detection, diagnostics, anticancer, therapeutics, catalysis, and microelectronics. However, there is still need for economic commercially viable as well as environmentally clean synthesis route to synthesize the silver nanoparticles (AgNPs). Silver is well known for possessing an inhibitory effect toward many bacterial strains and microorganisms commonly present in medical and industrial processes [2].

Green synthesis of metal nanoparticles is a growing research area because of their potential applications in nanomedicines. The synthesis of AgNPs using *Solanum villosum* leaves and its characterization is done using ultraviolet (UV), scanning electron microscopy (SEM), energy dispersive X-ray spectroscopy (EDX), and X-ray diffraction (XRD) analysis. *In vitro* cytotoxicity testing procedures reduce the use of laboratory animals. Hepatocellular carcinoma (HCC) is the fifth most common cancer in the world and the third most common cause of cancer death and accounts for 5.6% of all cancers [3].

The present study may open up several promising avenues of possible research. The *S. villosum* and related species are widely used as leafy herbs and vegetables, as a source of fruit and for various medicinal purposes. The *S. villosum* plant has been used in many ayurvedic medicines [4,5]. In spite of known uses in traditional medicines, no documental evidence is available on their biosynthesis of AgNPs and its activities. Hence, AgNPs of *S. villosum* are evaluated in a systematic manner to provide information for treating and preventing cancer and other diseases.

METHODS

Collection of plant material

The whole plant of *S. villosum* (Mill.) was collected from the Thadagam hills, Coimbatore district, southern India. The plant samples were identified and authenticated by the Botanical Survey of India (Southern part Coimbatore, Tamil Nadu, India). The identification No. BSI/SRC/5/23/2014-15/Tech/255. Various stages of plant, *S. villosum* is shown in the Fig. 1.

Preparation of aqueous extract of *S. villosum* leaves

The dried *S. villosum* leaves powder 10 g was boiled in 100 ml of distilled water for 10 minutes. The extract was cooled to room temperature filtered through Whatman No. 1 filter paper (Pore size 25 µm). The filtrate was further filtered through 0.6 µm sized filters.

Synthesis of AgNPs

The AgNPs were synthesized using a constant volume of the plant extract under various experimental conditions. Aqueous solution of 1 mM AgNO₃ was prepared and used for the synthesis of AgNPs. 5 ml of *S. villosum* aqueous extract is mixed with 95 ml of AgNO₃ for the synthesis of AgNPs. The formation of AgNPs is confirmed by color change from greenish to reddish brown. The appearance of reddish brown color after 3 hrs it indicates the formation of AgNPs.

Separation of AgNPs

The synthesized AgNPs were separated by centrifugation (Spectrofuge 7M) at 13,000 rpm for 15 minutes. The process was repeated by dispersion of pellets in water, to obtain colored supernatant solutions. The sample was then stored at -4°C for further use.

Characterization of AgNPs

UV-vis spectra analysis

The reduction of pure Ag⁺ ions was monitored by measuring the UV-vis spectrum of the reaction medium at 5 10-12 hrs. UV-Vis spectral analysis was done using UV-vis spectrophotometer UV- 2450 (Shimadzu).



Fig. 1: *Solanum villosum* (Mill.) plant

SEM

SEM analysis was done using Hitachi S-4500 SEM machine. Thin films of the sample were prepared on a carbon coated copper grid by just dropping a very small amount of the sample on the grid, extra solution was removed using a blotting paper and then the films on the SEM grid were allowed to dry by putting (placing) them under a mercury lamp for 5 minutes.

EDX

Energy dispersive X-ray analysis, the aqueous extract of *S. villosum* was dried and drop coated onto carbon film and performed on JEOL-MODEL 6390 SEM instrument equipped with a Thermo EDX attachments.

XRD analysis

The AgNPs solution obtained was purified by repeated centrifugation at 5000 rpm for 30 minutes followed by redispersion of the pellet of AgNPs into 10 ml of deionized water. After freeze drying of the purified silver particles, the structure and composition were analyzed by XRD and SEM. The dried mixture of AgNPs was collected for the determination of the formation of AgNPs by an X' Pert Pro X-ray diffractometer (PAN analytical BV, The Netherlands) operated at a voltage of 40 kV and a current of 30 mA with Cu K α radiation in a configuration.

In vitro cytotoxic effect of *S. villosum* AgNPs (SV-AgNPs) on HepG2 cell lines [6,7]

The human liver cancer cell line (HepG2) was obtained from the national center for cell science, Pune, and grown in eagles minimum essential medium containing 10% fetal bovine serum (FBS). All cells were maintained at 37°C, 5% CO₂, 95% air, and 100% relative humidity. Maintenance cultures were passaged weekly, and the culture medium was changed twice a week.

Cell treatment procedure

The monolayer cells were detached with trypsin-ethylene diamine tetra acetic acid to make single cell suspensions, and viable cells were counted by trypan blue exclusion assay using a hemocytometer. The cell suspension was diluted with medium containing 5% FBS to give final density of 1×10⁵ cells/ml. 100 μ l per well of cell suspension was seeded into 96-well plates at plating density of 10,000 cells/well and incubated to allow for cell attachment at 37°C, 5% CO₂, 95% air, and 100% relative humidity. After 24 hrs, the cells were treated with serial concentrations of the test samples. They were initially dispersed in phosphate buffered saline and diluted to twice the desired final maximum test concentration with serum-free medium. Additional four, 2-fold serial dilutions were made to provide a total of five sample concentrations. Aliquots of 100 μ l of these different sample dilutions were added to the appropriate wells already containing 100 μ l of medium, resulted the required final sample concentrations. Following drug addition, the plates were incubated for an additional 48 hrs at 37°C, 5% CO₂, 95% air, and 100% relative humidity. The medium containing without samples were served as control and triplicate were maintained for all concentrations.

$$\% \text{ Cell inhibition} = 100 - \frac{\text{Abs (sample)}}{\text{Abs (control)}} \times 100.$$

Nonlinear regression graph was plotted between % cell inhibition and log concentration, and inhibitory concentration at 50% (IC₅₀) was determined using GraphPad Prism software.

In vivo toxicity assessment of SV-AgNPs

Experimental animals

Healthy adult male Wistar albino rats weighing about 150-200 g were obtained from the small animal breeding center, Kerala Agricultural University, Mannuthy, Thrissur, Kerala, India. They were housed in polypropylene cages under the standard laboratory condition (25±2°C, humidity 60-70%, 12 hrs light/dark cycles). The animals were fed with commercial rat pellet diet (Sriram animal foods, Coimbatore, Tamil Nadu, India.) and water was provided ad libitum. The rats were acclimatized to laboratory conditions for 1 week before the commencement of the experiment. The animal care and handling were done according to the regulations of Council Directive CPCSEA no: 659/02/a about Good Laboratory Practice on animal experimentation. All animal experiments were performed in the laboratory according to the ethical guidelines suggested by the Institutional Animal Ethics Committee (IAEC).

Experimental design

To find out the toxicity effect of SV-AgNPs on male Wistar albino rats were carried out. In AgNPs, the IC₅₀ determined by MTT assay was used for fixing of different doses. After the adaptation period, the animals were divided into four groups with six animals in each group.

- Group I: Control.
- Group II: Rats fed with SV-AgNPs 100 μ g/kg body weight for 28 days.
- Group III: Rats fed with SV-AgNPs 200 μ g/kg body weight for 28 days.
- Group IV: Rats fed with SV-AgNPs 300 μ g/kg body weight for 28 days.

During the dosing periods, all the animals were observed daily for clinical signs and mortality patterns once before dosing, immediately after dosing and up to 4 hrs [8]. The body weight of each rat was assessed using a sensitive balance during the acclimatization period.

Hematological parameters

The hematological parameters such as hemoglobin packed cell volume, red blood cell, white blood cell, and platelet counts were assayed. The whole blood sample was analyzed for the changes in the blood cells using SYSMEX Xs-800 i (5 parts) automatic hematology analyzer.

Biochemical analysis

After the experimental regimen, the animals were sacrificed by cervical dislocation under mild chloroform anesthesia. The blood was collected in the centrifuge tubes, and serum was separated by centrifugation 2000 rpm for 20 minutes. The serum was used for the biochemical estimations such as aspartate transaminase (AST), alanine transaminase (ALT) [9], alkaline phosphatases (ALP) [10], and total protein [11] were assayed using various standard methods.

Histopathological studies

In the histopathological examination, the liver tissues were fixed in 10% formalin. The sections were cut into 3-5 μ m using microtome and processed for staining. Pathological changes in liver tissue were examined under light microscope [12].

Statistical analysis

Results were expressed as mean±standard deviation of six animals in each group. Statistical significance (p<0.05) was determined by one-way analysis of variance and *post-hoc* least significant difference test using SPSS 17 version.

RESULTS AND DISCUSSION

The biosynthesized AgNPs have been used for various drug delivery and drug carrier systems. AgNPs can be used for both active and passive targeting of drugs. The AgNP carrying small drug molecules or large biomolecules such as proteins, DNA, or RNA. Efficient release of these therapeutic agents to a target site for effective therapy.

In the present research work, biosynthesis of AgNPs from silver nitrate is one of the most widely used methods in the field of nanotechnology. During the biosynthesis, using the plant extract, the color of the

reaction medium changed rapidly from light greenish yellow to brown (Fig. 2a and b) due to surface plasmon resonance. This occurs due to the collective oscillations of the conduction electrons confined to metallic nanoparticles. The same mechanism was reported in ethanolic extract of leaves of *Pisonia grandis* [13]. It is well known that AgNPs exhibit a yellowish-brown color in aqueous solution due to excitation of surface plasmon vibrations in AgNPs. The approach employed in the production of these materials (AgNPs) is low cost and ecofriendly [14].

The major advantage of using plant extracts for the synthesis of AgNPs is that they are easily available, safe, and nontoxic, in most cases, have a broad variety of metabolites that can aid in the reduction of silver ions and are quicker than microbes in the synthesis. The main mechanism considered for the process is a plant-assisted reduction due to phytochemicals. The main phytochemicals involved are terpenoids, flavones, ketones, aldehydes, amides, and carboxylic acids [15].

The AgNPs were characterized by UV-Vis spectroscopy, one of the most widely used techniques and to confirm AgNPs formation by showing the plasmon resonance. The absorption spectrum of the AgNPs depicts in Fig. 3. The surface plasmon absorption band with a maximum of 200-800 nm, indicating the presence of AgNPs.

SEM has provided further insight into the morphological details of the synthesized AgNPs. SEM micrographs of the synthesized AgNPs using the aqueous extract of leaves of *S. villosum* fabricated on a glass substrate are shown in Fig. 4. The synthesized AgNPs were well dispersed without aggregation, possessing spherical shapes are confirmed by SEM.

In addition, elemental analysis of the synthesized AgNPs is further confirmed by EDX spectra with the absorption peak in the range of 3-4 keV (Fig. 5). This result is in accordance with the study of Jain *et al.* [16], who reported that the presence of optical absorption peak in the range

of 3-4 keV is typical for metallic silver nanocrystallites. While weaker peaks like C, O₂ and Cl are likely due to X-ray emission from proteins/sugars may be present in the *S. villosum* leaf extract.

In this, XRD pattern (Fig. 6) showed the conformation of the existence of peaks belonging to AgNPs in the sample. The Bragg's reflections were observed in XRD pattern at around $2\theta=28^\circ, 33^\circ$. Hence, the XRD pattern thus clearly illustrated that the AgNPs formed in this present synthesis. Peak obtained at around 33° indicated that the prepared samples were crystalline in nature. The crystalline size (D) was calculated using the Scherer's Debye formula from the full-width half maximum (FWHM).

$$D = \lambda / \beta \cos \theta$$

$$2\theta = 1.47897 / \beta \cos \theta \quad 33^\circ$$

$$= 1.47897 / 0.8386 = 17.63 \text{ nm.}$$

$$2\theta = 1.47897 / \beta \cos \theta \quad 28^\circ$$

$$= 1.47897 / 0.8829 = 16.75 \text{ nm}$$

Where, KD constant = 1.47897×10^{-10}

Where, D is the average crystallite domain size perpendicular to the reflecting planes. λ is the X-ray wavelength. β is the full width at half

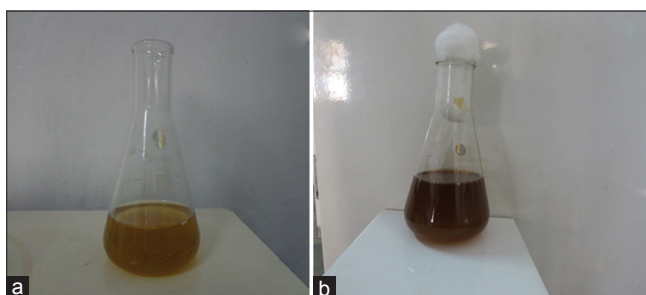


Fig. 2: (a) *Solanum villosum* aqueous leaf extract; (b) Color changes after adding silver nitrate reaction time of 10-12 hrs

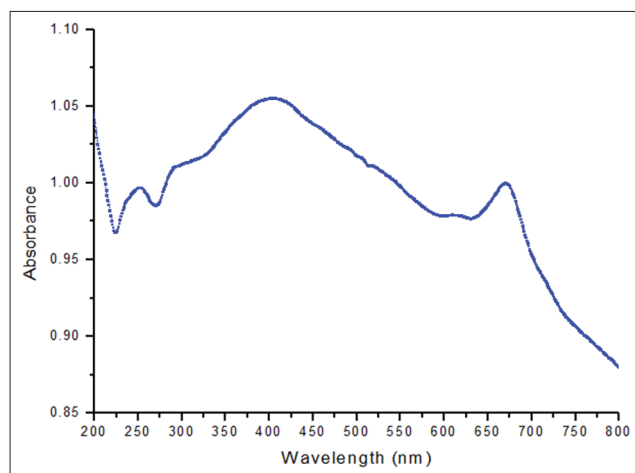


Fig. 3: Ultraviolet-visible spectra of *Solanum villosum* aqueous leaf extract reduction of silver nanoparticles

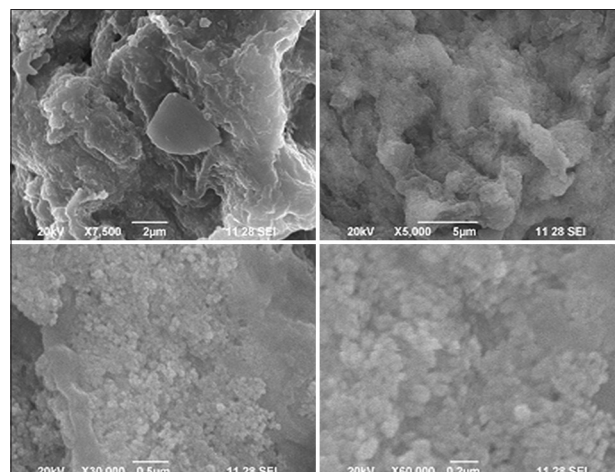


Fig. 4: Scanning electron microscopy micrographs for synthesized silver nanoparticles from aqueous leaf extract of *Solanum villosum*

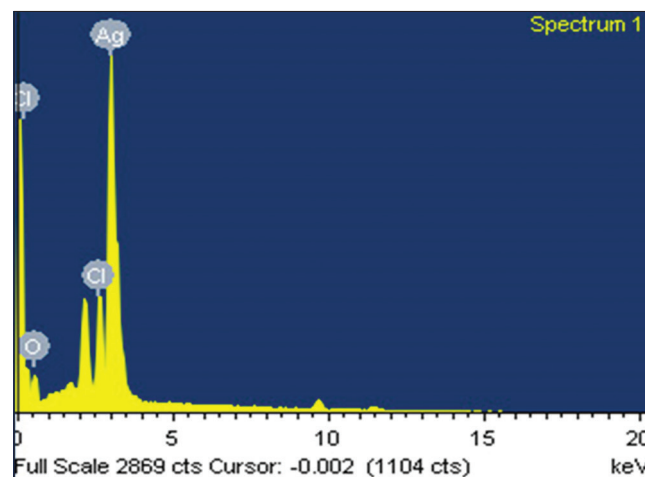


Fig. 5: Energy dispersive X-ray spectrum analysis for biosynthesized silver nanoparticles from aqueous leaf extract of *Solanum villosum*

maximum and θ is the diffraction angle. The crystalline size was found to be around 17.63 nm. AgNPs were synthesized by various plant materials as capping agents such as papaya [17] and neem [18].

In vitro cytotoxicity activity of SV-AgNPs

In this present research work, we have employed a dose-dependent approach to evaluate the toxicity of the biosynthesized AgNPs against the human HCC (HepG2) cell line. Evaluation of cytotoxicity in liver HepG2 cells by SV-AgNPs was performed using MTT assay (viability assay). HepG2 cell line was previously used for various anticancer studies. SV-AgNPs (1.88-30 $\mu\text{g}/\text{ml}$) in a dose-dependent manner as seen in the MTT assay. We observed AgNPs treatment (24 hrs incubation) significantly decreased the percentage of cell viability in HepG2 cells.

The proliferation of HepG2 cell was significantly inhibited by SV-AgNPs. Fig. 7 and Table 1 shows the changes in the percentage of cell viability treated with SV-AgNPs (1.88, 3.75, 7.5, 15, and 30 $\mu\text{g}/\text{ml}$) in HepG2 cells. There was 100% cell death at 30 $\mu\text{g}/\text{ml}$ concentration was observed. The IC_{50} was fixed as 8.34 $\mu\text{g}/\text{ml}$. AgNPs mainly react with cancer cells, it is selectively involved in disruption of the mitochondrial respiratory chain and leading to the production of ROS and interruption of ATP synthesis, which, in turn, cause DNA damage. Mainly, the plant *S. villosum* contains the phytochemicals and antioxidants exhibited the synergistic effect against the cancer cells. The synthesized AgNPs cause cell damage with unique morphological and biochemical hallmarks.

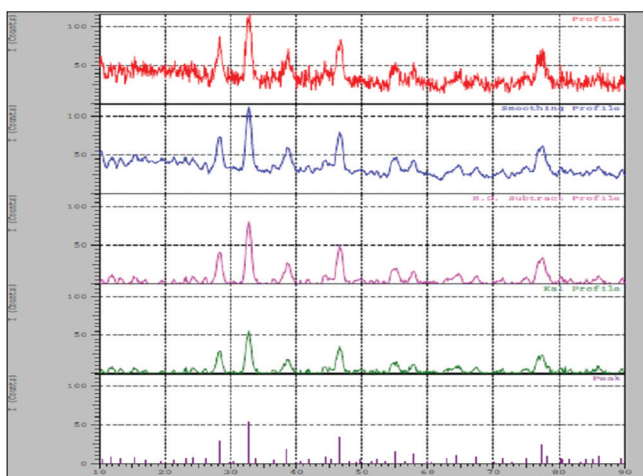


Fig. 6: X-ray diffraction spectrum analysis for synthesized silver nanoparticles from aqueous leaf extract of *Solanum villosum*

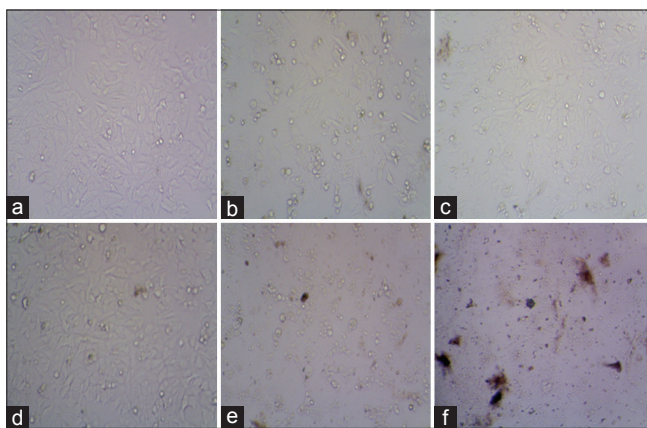


Fig. 7: In vitro cytotoxic activity of the biosynthesized *Solanum villosum* silver nanoparticles (SV-AgNPs) against HepG₂ cell line. (a) Untreated HepG₂ cell lines, (b) SV-AgNPs - 1.88 $\mu\text{g}/\text{ml}$, (c) SV-AgNPs - 3.75 $\mu\text{g}/\text{ml}$, (d) SV-AgNPs - 7.5 $\mu\text{g}/\text{ml}$ (e) SV-AgNPs - 15 $\mu\text{g}/\text{ml}$, (f) SV-AgNPs - 30 $\mu\text{g}/\text{ml}$

AgNPs from plant extract can interfere with the respiratory chain at the cytochromes and can interact with the electron transport chain to activate the intrinsic signaling pathway to cell death through the activation of downstream processing.

The cytotoxicity of these nanoparticles depends on their shape, size, surface chemistry, etc., as spherical AgNPs and microparticles are almost nontoxic to human alveolar epithelial cells [8]. AgNPs seemed to be a defense mechanism of protection from the highly reactive behavior of silver ions (Ag^+) to the cells. The incoming silver ions from the aqueous solution into the cells are converted to reduced state (Ag^0). The synthesis of nanoparticles by this reaction in cells is attributed to the presence of an enzyme called nitrate reductase. The enzyme is found to be present in both aerobes and anaerobes [19].

Toxicity assessment SV-AgNPs - in vivo study

Body weight and mortality changes

During the treatment of SV-AgNPs, all the animals were observed daily for clinical signs and mortality patterns. After administration of different doses from 100 μg , 200 μg , and 300 $\mu\text{g}/\text{kg}$ body weight, no clinical signs, mortality, and body weight changes of the rats. It is indicating the nontoxic effect of SV-AgNPs in minimum safety doses (Table 2).

Hematological and biochemical assays

In the repeated dose toxicity studies, administration of aqueous extract of SV-AgNPs in various experimental groups is carried out. All the groups did not produce any significant changes ($p < 0.05$) in hematological parameters and biochemical parameters are showed in the Tables 3 and 4. There were no harmful changes found in the level of AST, ALT, ALP, total protein in serum and hematological parameters in blood of treated groups (II, III, and IV) when compared with control (Group I). SV-AgNPs did not affect liver enzymes and blood cells, and the lack of significant alterations is a good indicator of liver functions and hematopoietic mechanism. Hence, it is clearly indicated that SV-AgNPs are nontoxic to normal rats.

Lovric *et al.* reported that after absorption of nanosilver from the gastrointestinal tract, entered to blood systemic circulation, therefore, this particle can, potentially, interact with different metabolites such as: Plasma proteins, coagulation factors, platelets, red and white blood cells. The smaller diameters of the nanoparticles are the more its influence and interact to cells and its intracellular mechanisms will increase [20].

Table 1: Effect of SV-AgNPs on HepG2 cell line (% inhibition)

Concentration of SV-AgNPs	% cell inhibition
1.88	-0.18
3.75	4.13
7.5	35.35
15	96.60
30	100

SV-AgNPs: *Solanum villosum* silver nanoparticles

Table 2: Body weight of the rats before and after 28 days of treatment with SV-AgNPs

Groups	Body weight (grams)	
	Before treatment	After treatment
Group I	210.00 \pm 5.47	219.00 \pm 3.74
Group II	208.33 \pm 6.83 ^{ns}	217.33 \pm 6.02 ^{ns}
Group III	209.17 \pm 4.91 ^{ns}	218.00 \pm 4.19 ^{ns}
Group IV	211.67 \pm 2.58 ^{ns}	220.33 \pm 2.33 ^{ns}

Values are expressed as mean \pm SD of six animals in each group. Statistical comparison: Group I versus Groups II, III, and IV. *Significant at 5% ($p < 0.05$), ^{ns}: Not significant, SD: Standard deviation, SV-AgNPs: *Solanum villosum* silver nanoparticles

AQ2

Table 3: Effect of SV-AgNPs on the hematological parameters in blood of control and experimental animals

Groups	Hb (g%)	PCV (%)	WBC ($10^3 \mu\text{l}$)	RBC ($10^{12} \mu\text{l}$)	Platelets ($10^9 \mu\text{l}$)
Group I	13.5±0.36	40.16±0.98	7.74±0.44	6.94±0.47	5.29±0.45
Group II	13.41±0.46 ^{ns}	40.16±1.47 ^{ns}	7.71±0.49 ^{ns}	6.90±0.32 ^{ns}	5.38±0.24 ^{ns}
Group III	13.36±0.36 ^{ns}	40.50±1.37 ^{ns}	7.70±0.41 ^{ns}	6.72±0.52 ^{ns}	5.49±0.36 ^{ns}
Group IV	13.41±0.33 ^{ns}	40.00±1.26 ^{ns}	7.90±0.53 ^{ns}	6.58±0.58 ^{ns}	5.66±0.41 ^{ns}

AQ2 Values are expressed as mean±SD of six animals in each group. Statistical comparison: Group I versus Groups II, III, and IV. *Significant at 5% ($p < 0.05$). ns: Not significant, WBC: White blood cell, PCV: Packed cell volume, RBC: Red blood cell, SV-AgNPs: *Solanum villosum* silver nanoparticles, Hb: Hemoglobin, SD: Standard deviation

Table 4: Effect of SV-AgNPs on liver function marker enzymes in serum of control and experimental animals

Groups	AST	ALT	ALP	Total protein
Group I	62±7.68	66.91±6.77	88±8.63	6.55±0.21
Group II	64±6.14 ^{ns}	66.88±3.97 ^{ns}	96±6.14 ^{ns}	6.43±0.31 ^{ns}
Group III	60±5.62 ^{ns}	66.43±1.82 ^{ns}	102±6.69 ^{ns}	6.35±0.38 ^{ns}
Group IV	63±6.21 ^{ns}	69.62±2.05 ^{ns}	108±6.99 ^{ns}	6.23±0.23 ^{ns}

AQ2 Values are expressed as mean±SD of six animals in each group. Statistical Comparison: Group I versus Groups II, III, and IV. *Significant at 5% ($p < 0.05$), ns: Not significant. Units: AST, ALT - μ moles of pyruvate liberated/L, ALP - μ moles of phenol liberated/L. Total protein - g/dl. AST: Aspartate transaminase, ALT: Alanine transaminase, ALP: Alkaline phosphatases, SD: Standard deviation, SV-AgNPs: *Solanum villosum* silver nanoparticles

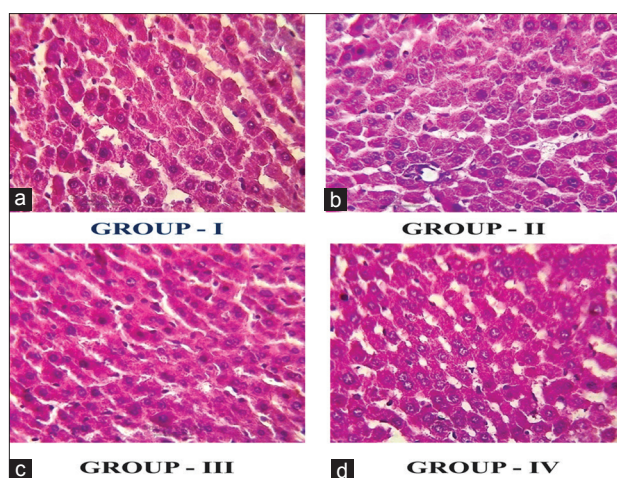


Fig. 8: Histopathology of liver (a) control, (b) *Solanum villosum* silver nanoparticles (SV-AgNPs) - 100 $\mu\text{g}/\text{kg}$ body weight, (c) SV-AgNPs - 200 $\mu\text{g}/\text{kg}$ body weight, (d) SV-AgNPs - 300 $\mu\text{g}/\text{kg}$ body weight

Histopathological investigations

All the control and experimental animals showed the normal architecture (Fig. 8) of the liver with central vein and cords of hepatocytes radiating from the central vein indicating the hepatoprotective activity. There was no cellular injury which indicates that the SV-AgNPs have no side effect at all the doses tested. The evaluation of histopathological changes in organs remains a cornerstone in safety assessment of medicines [21].

AgNPs synthesized from medicinal plant *S. villosum* and evaluated toxicity for HepG2 cell lines. The AgNPs significantly decreased the cell viability of HepG2 cells but did not cause any changes in the normal healthy rats. Nanoparticles of larger size have proven to be toxic to the cells. Larger size nanoparticles also do not bind with the specific receptors. The smaller size (5-20 nm) of the nanoparticle can easily interact with cancer cells cause damage. This particle size range has proven to be less toxic to the cells and also exhibit higher binding affinity toward the receptors. Similar results have been obtained when the particles were checked for interaction with HIV-1 [22]. Another reason,

binding of AgNPs only with cancer cells but not the other body cells. One possible reason could be due to morphological and biochemical reaction differences between cancer cells and the other body cells.

The previous study reported that nanoparticle has difference in the curvature of the different-shaped nanoparticles. For example, the rod-shaped nanoparticles can have a larger contact area with the cell membrane receptors than the spherical nanoparticles when the longitudinal axis of the rods interacts with the receptors. The cancer cells are different in pore size when compared to the other normal cells and so a size controlled targeting of AgNPs can prove effective in the case of cancer treatment [23].

Current cancer treatments include surgical intervention, radiation and chemotherapeutic drugs, which often also kill healthy cells and cause toxicity to the patient [24]. The smaller size particles are attributed to the stability, catalytic activity, and enhanced adherence to the cells. Previous reports suggest that the increase in the concentration of AgNPs has resulted in the increase in cell death [25,26]. The effects of AgNPs on size-dependent toxicity with various concentrations already explained earlier [27].

CONCLUSION

The biological method of synthesis of AgNPs from *S. villosum* has proved to be an ecofriendly method than the chemical methods. The physical and chemical method involves use of hazardous chemicals and highly expensive approaches. The role of AgNPs is an anticancer agent in the field of medicine. The use of nanoparticles revealed that decrease the use of expensive drugs for cancer treatment. So, the use of AgNPs for cancer treatment is the novel and effective approach in the field of cancer biology. In conclusion, SV-AgNPs have anticancerous activity; it enhances the apoptotic property. Further studies on the mechanisms of AgNPs and the new drug discovery for synthesized AgNPs of the *S. villosum* for medical and other industrial application. However, further *in vivo* studies are needed to fully characterize the antiproliferative potential of the biosynthesized AgNPs against HCC.

ACKNOWLEDGMENT

The authors wish to acknowledge Indian Council of Medical Research (ICMR) for their financial assistance for this Senior Research Fellowship (Grant No. 45/62/2013/BMS/TRM/Dt 5.12.2014), Government of India, New Delhi, is gratefully acknowledged.

REFERENCES

1. Kaviya SS, Viswanathan B. Green synthesis of silver nanoparticles using *Polyalthia longifolia* leaf extract along with D-Sorbitol. *J Nanotech* 2011;2011:1-5.
2. Jiang HM, Wong AC, Denes FS. Plasma enhanced deposition of silver nanoparticles onto polymer and metal surfaces for the generation of antimicrobial characteristics. *J Appl Polym Sci* 2004;93:1411-22.
3. Nahum MS, Ezequiel R, Alves DM, Norberto C, Chavez T. Clinical practice guidelines: Management of hepatocellular carcinoma. *Ann Hepatol* 2014;13(1):4-40.
4. Yesodharan K, Sujana KA. Wild edible plants traditionally used by the tribes in the Parabikulam Wildlife Sanctuary, Kerala, India. *Nat Prod Radiance* 2007;6(1):74-80.
5. Venkatesh R, Vidya R, Subbaiyan B, Samyudurai P, Kalaivani K.

- Phytochemical studies on the alkaloids of medicinally important plant *Solanum villosum* (Mill) using HPTLC. Int J Pharm Res Sci 2014;2(3):247-54.
6. Mosmann T. Rapid colorimetric assay for cellular growth and survival: Application to proliferation and cytotoxicity assays. J Immunol Methods 1983;65(1-2):55-63.
 7. Monks A, Scudiero D, Skehan P, Shoemaker R, Paull K, Vistica D, *et al.* Feasibility of a high-flux anticancer drug screen using a diverse panel of cultured human tumor cell lines. J Natl Cancer Inst 1991;83(11):757-66.
 8. Saidu Y, Bilbis LS, Lawal M, Isezuo SA, Hassan SW, Abbas AY. Acute and sub-chronic toxicity studies of crude aqueous extract of *Albizia chevalieri* Harms (Leguminosae). Asian J Biochem 2007;2:224-36.
 9. Reitman S, Frankel SA. Colorimetric method for the determination of serum glutamic oxaloacetate and glutamic pyruvic transaminase. Am J Clin Pathol 1957;28:56-63.
 10. King E, Armstrong AR. Determination of serum and bile phosphatase activity. Can Med Assoc J 1934;31:376.
 11. Lowry OH, Rosenbrough RN, Farr AL, Randall RJ. Protein measurement with the folin phenol reagent. J Biol Chem J 1957;193:265-75.
 12. Kleiner DE, Brunt EM, Van Natta M, Behling C, Contos MJ, Cummings OW, *et al.* Design and validation of a histological scoring system for nonalcoholic fatty liver disease. Hepatology 2005;41(11):1313-21.
 13. Parashar V, Parashar R, Sharma B, Pandey AC. Biomimetic synthesis of nanoparticles: Science, technology and applicability. Digest J Nanomat Biostru 2009;4(1):45-50.
 14. Sukumaran P, Eldho KP. Silver nanoparticles: Mechanism of antimicrobial action, synthesis, medical applications, and toxicity effects. Int Nano Lett 2012;2:32.
 15. Choi Y, Ho N, Tung C. Sensing phosphatase activity by using gold nanoparticles. Chem Int Ed 2007;707:46.
 16. Jain D, Kumar DH, Kachhwaha S. Synthesis of plant-mediated silver nanoparticles using papaya fruit extract and evaluation of their antimicrobial activities. Digest J Nanopart Biostruc 2009;4:263-557.
 17. Shankar SS, Rai A, Ankamwar B, Singh A, Ahmad A, Sastry M. Biological synthesis of triangular gold nanoprisms. Nat Mater 2004;3(7):482-8.
 18. Anila L, Vijayalakshmi NR. Flavonoids from *Embllica officialis* and *Mangifera indica*-effectiveness for dyslipidemia. J Ethnopharmacol 2002;79(1):81-7.
 19. Ahmad A, Mukherjee P, Senapati S, Mandal D, Khan MI, Kumar R. Extracellular biosynthesis of silver nanoparticles using the fungus *Fusarium oxysporum*. Coll Surf B Biointerf 2003;28:313-8.
 20. Lovric J, Bazzi HS, Cuie Y, Fortin GR, Winnik FM, Maysinger D. Differences in subcellular distribution and toxicity of green and red emitting CdTe quantum dots. J Mol Med (Berl) 2005;83(5):377-85.
 21. Greaves P. Histopathology of Preclinical Toxicity Studies: Interpretation and Relevance in Drug Safety Evaluation. 3rd ed. New York: Academic Press; 2007.
 22. Elechiguerra JL, Burt JL, Morones JR, Bragado AC, Gao X, Lara HH. Interaction of silver nanoparticles with HIV-1. J Nanobiotechnol 2005;3:1-10.
 23. Pickup JC, Zhi ZL, Khan F, Saxl T, Birch DJ. Nanomedicine and its potential in diabetes research and practice. Diabetes Metab Res Rev 2008;24(8):604-10.
 24. Peer D, Karp JM, Hong S, Farokhzad OC, Margalit R, Langer R. Nanocarriers as an emerging platform for cancer therapy. Nat Nanotechnol 2007;2(12):751-60.
 25. Kalishwaralal K, Banumathi E, Pandian SB, Deepak V, Muniyandi J, Eom SH, *et al.* Silver nanoparticles inhibit VEGF induced cell proliferation and migration in bovine retinal endothelial cells. Colloids Surf B Biointerfaces 2009;73(1):51-7.
 26. Hsin YH, Chen CF, Huang S, Shih TS, Lai PS, Chueh PJ. The apoptotic effect of nanosilver is mediated by a ROS- and JNK-dependent mechanism involving the mitochondrial pathway in NIH3T3 cells. Toxicol Lett 2008;179(3):130-9.
 27. Carlson C, Hussain SM, Schrand AM, Braydich-Stolle LK, Hess KL, Jones RL, *et al.* Unique cellular interaction of silver nanoparticles: Size-dependent generation of reactive oxygen species. J Phys Chem B 2008;112(43):13608-19.

Author Queries???

AQ2: Kindly cite significant value (*) in the Table Part